Biophysical Chemistry 19 (1984) 171–181
Elsevier

BPC 00846

A NEW THEORETICAL INDEX OF BIOCHEMICAL REACTIVITY COMBINING STERIC AND ELECTROSTATIC FACTORS

AN APPLICATION TO YEAST $tRNA^{Phe}$

Richard LAVERY and Alberte PULLMAN

Institut de Biologie Physico-Chimique, Laboratoire de Biochimie Théorique associé au CNRS, 13, rue Pierre et Marie Curie, 75005 Paris, France

Received 13th October 1983
Accepted 2nd January 1984

Key words: Yeast $tRNA^{Phe}$; Reactivity; Electrostatic field; Accessibility

A new theoretical index of the chemical reactivity of sites within macromolecules is developed, which combines both steric and electrostatic factors. It is applied to the study of yeast $tRNA^{Phe}$ and the results obtained are compared with known experimental reactivities. A comparison indicates the superiority of the new index over the sole use of the surface accessibility.

1. Introduction

Since the development of quantitative calculations of atomic steric accessibilities in molecules and macromolecules [1–5] and their initial application to solvent binding (see, for example, refs. 6–8), it has been suggested that they might also be used more generally as a guide to chemical reactivity [5,9–11]. Although this seems justifiable on the basis of a simple kinetic interpretation of chemical reactions, namely, the more exposed an atom is, the more likely it is to come into contact with a reactive species, it must not be forgotten that the electronic properties of the target atom are also of primordial importance in determining whether or not a reaction occurs. A very clear example which indicates the necessity of accounting for the latter factor is given by the interaction of the purine and pyrimidine bases of DNA with electrophilic species: thus, in passing from the free bases to nucleotides, to single-stranded DNA and finally to double-stranded DNA one observes, not surprisingly, a decrease in atomic accessibilities [5] while, in the majority of cases, the reactivity increases (see references cited in refs. 12 and 13). Work carried out in this laboratory has been able to show that there is a relation between this increasing reactivity and the increasing values of the molecular electrostatic potentials at the reactive sites in successively larger DNA fragments [12,13].

Further, detailed studies of different conformations of DNA [12–14] and of yeast $tRNA^{Phe}$ [9,10,15] have shown that within these macromolecules the steric and electronic (in particular potential and field) characteristics of a given type of base reactive site are highly dependent on its surroundings. This is particularly true for irregular structures such as that of the transfer ribonucleic acid. It is therefore inevitable that both steric and electronic properties must be considered together if a site reactivity is to be explained. Attempts at such a simultaneous consideration of these two factors have already been made by us [10,12] in the form of two-dimensional potential/accessibility graphics for many sites in yeast $tRNA^{Phe}$. However, it would be desirable to achieve

0301-4622/84/$03.00 © 1984 Elsevier Science Publishers B.V.

a closer combination of the two properties by generating a single index which contains both aspects.

How best can such a combined index be obtained? Since atomic accessibility can be considered as a measure of the kinetic probability of contact between a target atom and an attacking species, it seems reasonable to associate with it a similar kinetic measure of the electronic properties. In the case of charged or highly polar attacking species, which will be the principal object of our interest, this can be achieved by using the electrostatic field in the proximity of the target which will, to a first approximation, determine the force pulling the attacking species towards (or pushing it away from) the site of binding. Consequently, it is this property that we shall use in elaborating the reactivity index described in the following section.

At the same time we will also reconsider the calculations of accessibility, examining to what extent it is possible to justify the usual approximation of these calculations, namely, treating polyatomic attacking species as simple spheres and we will show how the radius of such model spherical probes may be obtained quantitatively.

2. Methods

In order to calculate the accessibility of atoms within macromolecules we employ the concept originally developed by Lee and Richards [1,2] which consists of rolling a spherical probe over the van der Waals surface of a macromolecule and determining, for a given atom, the positions of the probe which do not lead to its intersection with the van der Waals spheres of any of the other atoms of the macromolecule (fig. 1). In this framework, the accessibility of the atom concerned can be expressed either as a 'contact surface area' (CSA) which is the accessible area on the surface of the van der Waals sphere (radius r_i) of the target atom in the macromolecule or as a 'surface accessible area' (SAA) which is the corresponding accessible area on the surface of a sphere of radius equal to that of the target atom plus that of the probe ($r_i + r_a$), i.e., the area covered by the locus

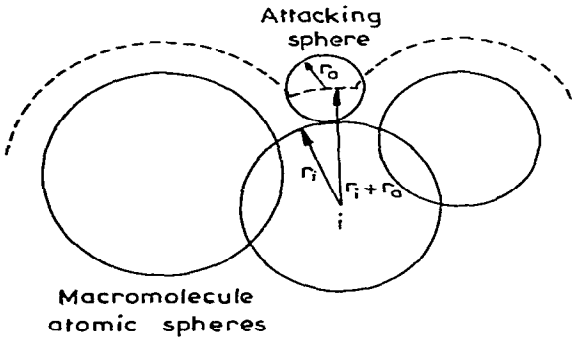

Fig. 1. Sphere radii involved in the calculation of accessibility.

of the center of the attacking sphere for the accessible positions of the probe. It is the SAA which is generally computed by a geometrical algorithm developed by Lee and Richards, which limits the treatment to simple spherical probes whose radii are either chosen arbitrarily or at best by an empirical search for an 'effective' value which yields the best correlation with experimental results on the reactivity of the reagent considered [11].

We have developed an alternative technique [5] which opens the way to treating explicitly polyatomic species. This approach requires covering the van der Waals sphere of the target atom of the macromolecule with a grid of uniformly distributed points, generated by the Korobov technique [19]. The attacking species, say, to start with, a sphere of chosen radius, is then placed in contact with each of the grid points and it is checked whether it intersects any of the van der Waals spheres of the other atoms composing the macromolecule. If no such intersections exists, the associated grid point is classed as accessible. The fraction of the total number of grid points which lead to accessible positions of the probe may be used directly as a measure of the accessibility of the target atom. Alternatively, it may be multiplied by the area of a sphere of radius r_i to obtain the CSA, or by the surface area of a sphere of radius ($r_i + r_a$) to obtain the SAA. Note that the two values are related by the simple equation:

$$\mathrm{SAA} = \mathrm{CSA}\left(\frac{r_i + r_a}{r_i}\right)^2$$

The extension of this technique for the explicit treatment of polyatomic attacking species is straightforward [5]. The polyatomic species is now also surrounded by its appropriate van der Waals surface. One of its atoms is chosen to be in contact with the macromolecular target atom and a grid of points is inscribed on its surface, similar to that on the target atom. By placing successively each of these points in contact with each of the grid points of the target and, in addition, performing, at each step, a rotation of the attacker around the axis joining the centers of the spheres of the attacker and target atoms, all possible orientations of the attacker molecule can be tested for their accessibility. The overall accessibility of the chosen target atom can be expressed as a fraction representing the number of accessible orientations found divided by the total number tried.

The use of such a developed representation of the attacking species is necessarily more complex than that of a simple sphere. We shall therefore consider in the following section to what extent it is nevertheless possible, on the basis of the results obtained with the developed representations, to describe a polyatomic reagent by a single sphere with a quantitatively determined radius.

In view of combining the accessibility with the macromolecular field which acts upon the attacking species, it seems most reasonable to employ the field at the center of the attacking sphere for each of its accessible positions. (These points correspond to the locus discussed above). We then propose to define as an index of reactivity the quantity obtained by a numerical integration of the field over the corresponding SAA generated by the center of the probe. In order to achieve a distinction between atoms which are attractive or repulsive towards electrophiles we replace the net field at each point by its projection on the radius vector ($\vec{r}$) joining the center of the attacked atom of the macromolecule to the current position of the center of the attacking sphere, so that the index is given by:

$$\int_S \vec{F}\cdot\vec{r}_u \cdot ds$$

where S is the SAA defined earlier and $\vec{r}_u$ a unit vector along the direction $\vec{r}$.

With this definition, if the electrostatic field is more or less aligned with the radius vector and pointing outwards from the attacked atom concerned, this atom will be repulsive towards positively charged electrophiles and the resulting integral will be positive. If, conversely, the field is again more or less aligned with the radius vector but points towards the atom of the macromolecule, this atom will be attractive towards positively charged electrophiles and the resulting integral will be negative. Finally, if the field is more or less perpendicular to the radius vector the resulting integral will be small, corresponding to an atom which is unlikely to react, since the ambient field will slide a charged attacking species towards a neighboring atom which is a stronger field source. We will term the resulting index ASIF, signifying 'Accessible Surface Integrated Field'. Its values will be expressed in units of V Å.

It may be remarked that the ASIF index represents, in fact, the flux of the electrostatic field through the accessible surface described and hence may be expressed in units of electronic charge. The factor of conversion between V Å and electronic charge is 5.5266×10^{-3}.

Since the area covered by the locus of the attacking sphere can be quite large, a high number of points in the Korobov grid is required to obtain precise values. We have employed almost 1000 points (exactly, 987).

The size of yeast $tRNA^{Phe}$ (2513 atoms) makes calculations of electrostatic fields by our usual OMTP multipole expansion [20,21] very time-consuming, particularly for the high grid densities presently necessary. This technique has also necessitated, in our preceding studies, a grouping of conformationally similar phosphates and sugars [22,23] in order to minimize the number of ab initio wave functions to be calculated. We have consequently developed an optimized monopole representation by reparameterizing the Hückel-Del Re procedure [24,25] in order to obtain a good fit to the OMTP potentials, fields and ASIF values for the nucleic acid subunits. This representation, which is detailed elsewhere [26], was tested for $tRNA^{Phe}$ using the same subunit conformations as in our OMTP studies and was found to give very satisfactory results. It has the advantage of per-

mitting more rapid calculations, avoiding the grouping of subunits and also allowing for charge redistribution between the constituent subunits of the macromolecule by calculating the charges for each subunit within a medium-sized nucleic acid fragment rather than simply for the isolated subunit itself (see ref. 26 for details). The coordinates used for $tRNA^{Phe}$ are those of ref. 27.

3. Results and discussion

3.1. A sphere as a model for polyatomic attacking species

We begin by considering the justification for the use of a sphere, and the determination of an appropriate radius for representing a given polyatomic attacking species. In order to test such modeling we have calculated the accessibility of a number of different polyatomic reactants: (a) a methyl cation, (b) an ethyl cation, (c) a phenyl cation and (d) a *tert*-butyl cation, each being treated explicitly as polyatomic, towards a selection of different reactive sites within yeast $tRNA^{Phe}$. We will consider here the results for N7 of guanine, C8 of guanine, N3 of adenine and O2 of cytosine. By studying this variety of sites for all such bases in $tRNA^{Phe}$ we can be reasonably confident that if a spherical model of the polyatomic species considered can be shown to reproduce well all the corresponding polyatomic accessibilities it should also be appropriate for subsequent studies involving other sites in this or in other macromolecules.

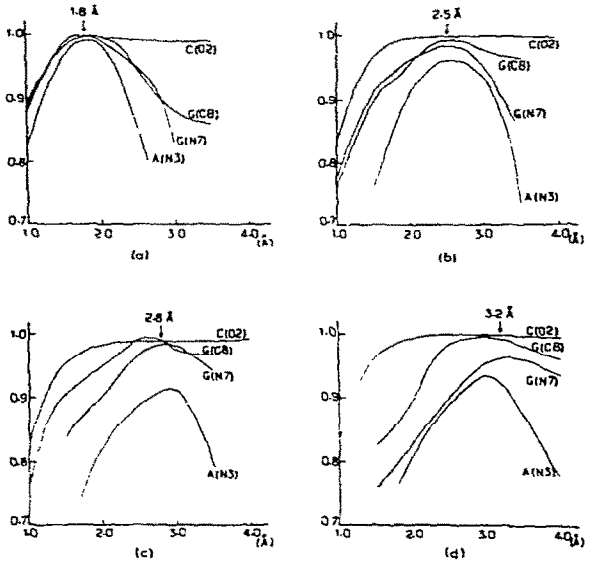

Fig. 2. Spherical model vs. explicit polyatomic model for calculating accessibility of: (a) methyl cation, (b) ethyl cation, (c) phenyl cation, (d) *tert*-butyl cation. The vertical axis in each figure gives the correlation factor between the true polyatomic accessibility and the model sphere accessibility; the corresponding sphere radii are indicated along the horizontal axis.

The results for the spherical modelling of these cations are shown in fig. 2a–d. The abscissae of these graphs indicate the radius of the sphere modeling the polyatomic species, while the ordinate shows the correlation factor obtained between the spherical accessibility and the polyatomic accessibility for the set of sites studied within yeast $tRNA^{Phe}$. The four curves in each figure are labelled to show the type of base target atom to which they refer. From the results in fig. 2a it is clear that the rather small and spherical methyl cation can be modeled very successfully by a sphere with an optimal radius of 1.8 Å. It is interesting to note that the quality of the correlation obtained at this radius is almost equally good for all the types of base site despite their very different environments. It may also be remarked that sites such as C8 of guanine, for which many residues have only moderate accessibilities, require a finer adjustment of the radius of the attacking sphere than do sites such as O2 of cytosine, for which there are a few highly accessible residues, while the majority are inaccessible.

The results for the remaining polyatomics, the ethyl cation (fig. 2b), the phenyl cation (fig. 2c) and the *tert*-butyl cation (fig. 2d) show that, even with these larger species, good spherical models can also be obtained with radii of 2.5, 2.8 and 3.2 Å, respectively. It is clear, however, that with the increasing size of the species considered, the quality of the optimal correlation decreases somewhat and that the accordance between the optimal radii for each type of base site also becomes somewhat less satisfactory. Nevertheless, it seems that, over-

all, a spherical model can be quite successful for species of the complexity considered here, provided, however, that its radius is appropriately chosen.

On the basis of these findings we shall use accurate spherical probes with justified radii, for the studies of the reactivity of $tRNA^{Phe}$ in the examples which follow, when the nature of the attacking species is known. For the examples where this is not the case, we have studied a range of possible radii and we discuss the influence of this variation on the correlations subsequently obtained.

We will now present the comparison of the calculated values of the newly proposed ASIF index and the experimentally observed reactivities of yeast $tRNA^{Phe}$ for the four principal types of base and also for the phosphates. At the same time we will analyze the indications of reactivity obtained by using only accessibilities, which have previously been advocated by certain authors as a sufficient measure.

3.2. Reactivity of guanines in $tRNA^{Phe}$

Three electrophilic reagents attacking guanines in yeast $tRNA^{Phe}$ have been studied: dimethylsulfate [28] which methylates the N7 position, kethoxal which reacts by bridging the N1 and amino N2 positions [29] and carbodiimide which forms an adduct at N1 [30]. The results for the first of these reagents are given in fig. 3. In this figure and in those which follow (figs. 5–11), the accessibility (expressed as surface-accessible areas, SAA) and ASIF values calculated for the appropriate atoms of the residues concerned are shown on vertical scales on the left- and right-hand sides, respectively. The residues are numbered following the nucleotide sequence in yeast $tRNA^{Phe}$. The experimental results are indicated by three symbols: (○) for unreactive residues, (●) for reactive residues and (◑) for partially reactive residues. The attacking sphere radius employed for this reaction, which involves the addition of a methyl cation, was 1.8 Å, the value obtained in the preceding section.

It can be seen from fig. 3 that six guanines (nos. 18, 19, 30, 34, 45 and 71) are fully methylated and

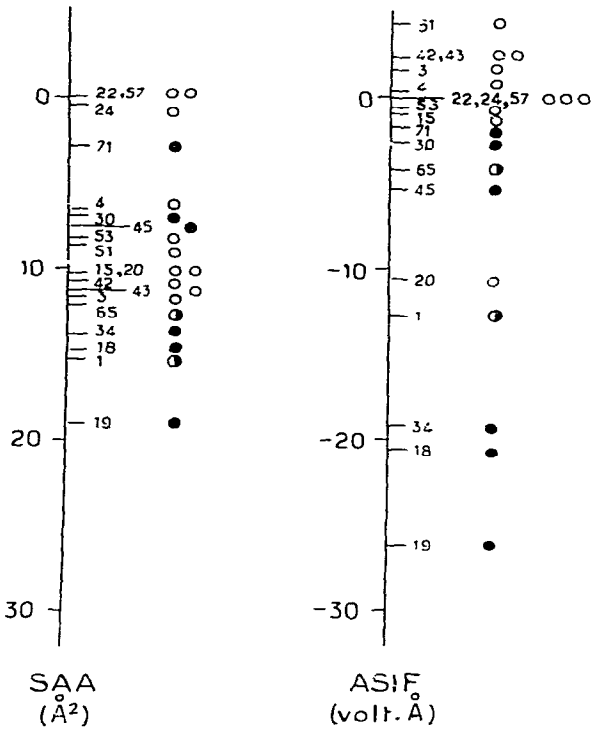

Fig. 3. Accessibility and ASIF for N7 of guanine in $tRNA^{Phe}$. Symbols represent reactivity towards dimethyl sulfate. In this figure and in figs. 5–11 the numbers refer to the nucleotide positions in yeast tRNA and the symbols indicate the experimental reactivities: (●) reactive, (◑) partially reactive and (○) unreactive.

that two are partially reactive (nos. 1 and 65). The left-hand scale shows that the accessibility of these bases for the appropriate radius of the attacking sphere does not account well for the experimental results. Other authors [11] have advocated a much larger effective sphere radius of 3.5 Å for this reactant and, although we do not think that such a value can now be justified, we have calculated the guanine N7 accessibilities for a wide range of radii to see whether the resulting correlation can be improved. The results are shown in fig. 4 from which it is clear that the reactive bases (indicated by dotted lines) and the unreactive bases (indicated by full lines) are not well separated from one another at any of the radii investigated.

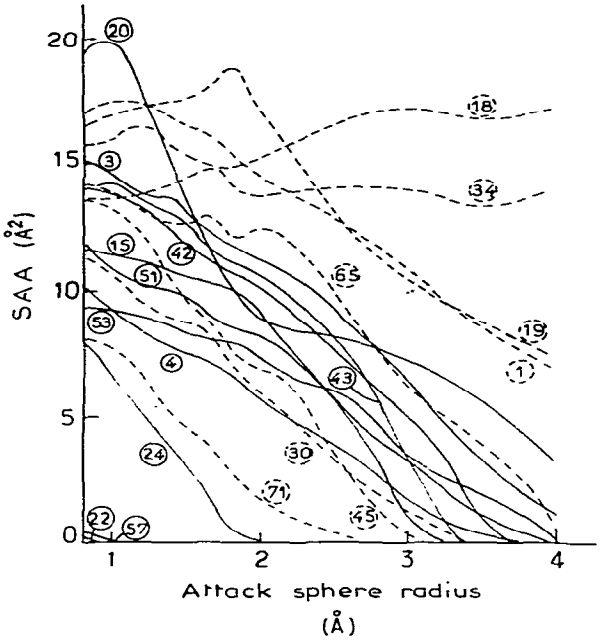

Fig. 4. Accessibility of the N7 of guanine sites in $tRNA^{Phe}$ for a range of radii of the attacking sphere.

In contrast, when electrostatic effects and accessibilities are both taken into account, by using the ASIF index, a much better correlation is achieved. With the sole exception of guanine 20, all the reactive and partially reactive residues are now grouped together at more negative ASIF values. This improvement shows that the inclusion of electrostatic effects is vital to obtain a satisfactory correlation with reactivity. Moreover, because of the very good overall correlation achieved, we may reasonably assume that the inactivity of guanine 20 is due to an effect not included in our present methodology, possibly a conformational change of the macromolecule in solution or a specific counterion interaction.

The second reaction of guanine studied is that with kethoxal. This reagent bridges two sites, N1 and N2, and we must consequently consider the ASIF values of both targets. The choice of an accurate attacking sphere radius is not possible in this case and we will consequently consider both accessibility and ASIF results over a range of radii, from 2 to 4 Å. Thus, in fig. 5 and the related figures which follow, the results for each base are shown by curves, the left-hand extremity of which corresponds to an attacking sphere radius of 2 Å, the value on the axis to a radius of 3 Å and the right-hand extremity to a radius of 4 Å. Note that in the case of these targets and for other hydrogen-bearing ring or amino nitrogens, we have calculated what may be termed 'group' accessibility and ASIF values by adding together the results for the nitrogens and their bound hydrogens, since this appeared to give a better image of the target site, the accessible surface of the nitrogen atom alone often being very small.

The results for N2 of guanine in fig. 5 show

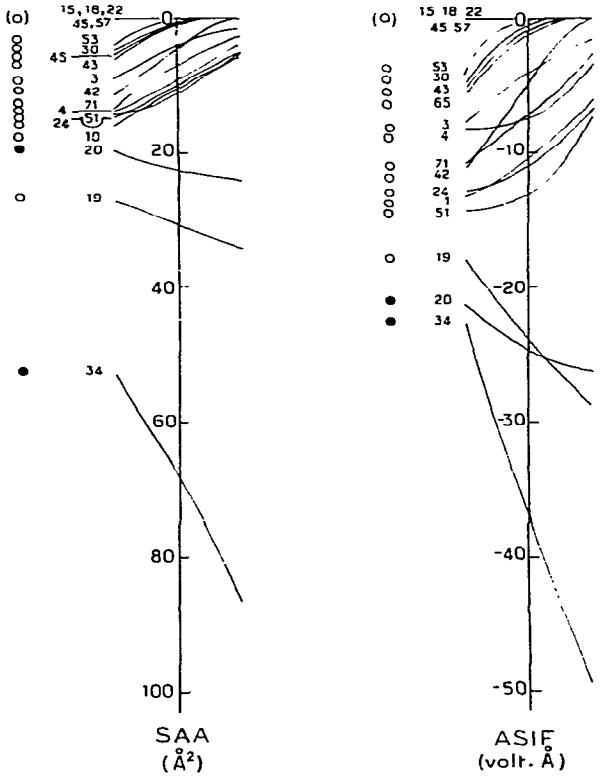

Fig. 5. Accessibility and ASIF for N2 of guanine in $tRNA^{Phe}$. Symbols represent reactivity towards kethoxal.

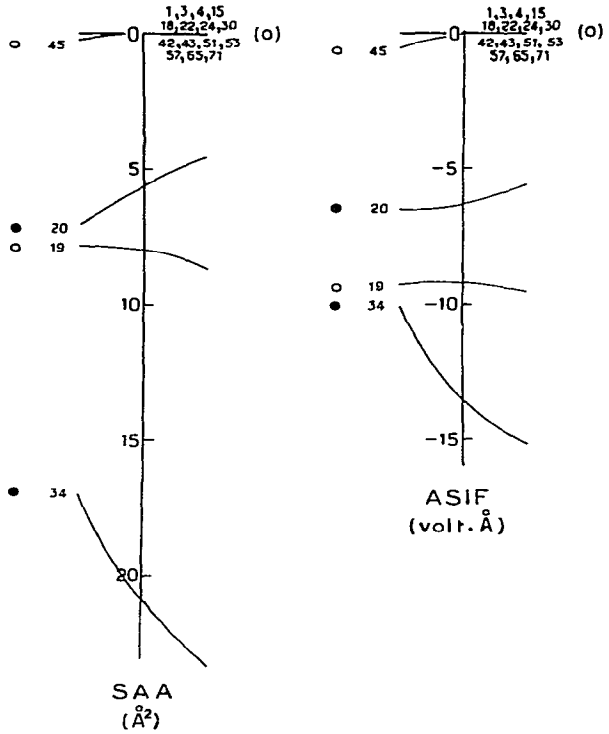

Fig. 6. Accessibility and ASIF for N1 of guanine in $tRNA^{Phe}$. Symbols represent reactivity towards carbodiimide.

that three residues have large accessibilities, guanines 20 and 34, which are reactive, and, placed in between, guanine 19 which is not. The ASIF values are most negative for the two reactive residues up to attack radii of 3 Å, but beyond this values guanine 19 becomes more negative than guanine 20.

Fig. 6 shows the results for the N1 atom of guanine, from which bases 19, 20 and 34 are seen to be the only ones with large values in terms of either accessibility or ASIF. In both cases the unreactive guanine 19 has values between those of the two reactive bases for all the attack radii studied. Its lack of reactivity may thus be due to its unfavorable ASIF value at the N2 site for smaller attacking spheres or perhaps due to the fact that unlike guanines 20 or 34 or any of the other fully reactive sites presently discussed it is involved in a hydrogen bond which should presumably be disrupted for the reaction with kethoxal to occur. The same situation prevails in the case of the reaction of guanine with carbodiimide at N1 (for which it is again necessary to study a range of attacking spheres), residues 20 and 34 alone being reactive, as shown by the symbols in fig. 6.

3.3. *Reactivity of adenines in $tRNA^{Phe}$*

The first reaction involving adenine that we shall consider is that with monoperphthalic acid which induces the formation of an N1-oxide [31] via the reactive intermediate OH^+ [32]. Preliminary study showed that the accessibility for this diatomic species could be very well reproduced by a sphere of 1.5 Å radius which is consequently the value we now employ. The calculated indices for N1 are given in fig. 7. Four bases are known to be reactive (nos. 35, 36, 38 and 76) and

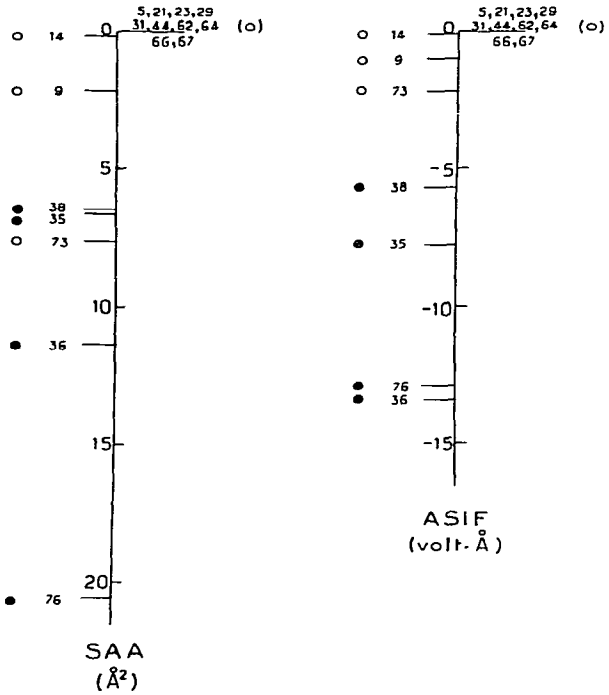

Fig. 7. Accessibility and ASIF for N1 of adenine in $tRNA^{Phe}$. Symbols represent reactivity towards monoperphthalic acid.

these are also found to be well grouped at the strongest negative ASIF values. The accessibility alone, on the other hand, exhibits an inversion in the ordering, placing the unreactive adenine 73 at a higher value than the reactive bases 35 and 38.

The second reagent tested with adenine is diethyl pyrocarbonate [28] which normally carboethoxylates the N7 site. The bases in yeast $tRNA^{Phe}$ were not found to be reactive towards this reagent, but adenine 76 was not assayed. We again considered a range of attacking sphere radii for this rather complicated reagent. The results in fig. 8 show that at all radii only one residue has a large accessibility, or strongly negative ASIF value, adenine 76. It would seem reasonable to suppose that this base may in fact be reactive towards diethyl pyrocarbonate.

The third reaction involving adenine is that with 1-fluoro-2,4-dinitrobenzene which is presumed to interact by substitution at N6, although

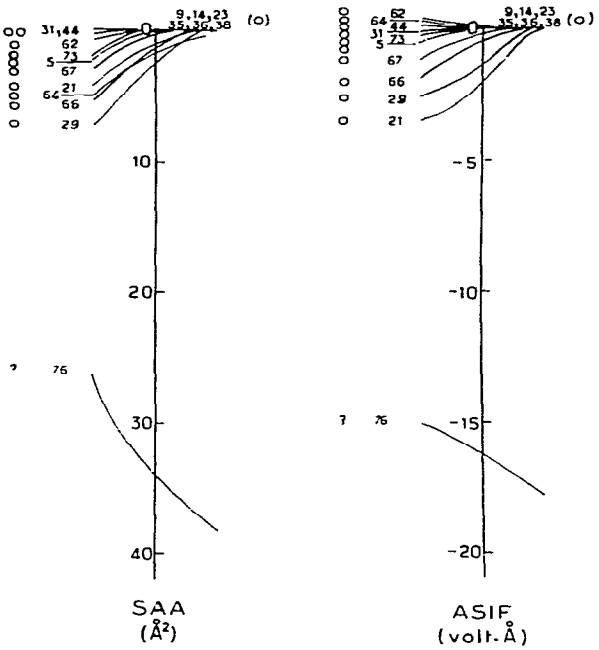

Fig. 8. Accessibility and ASIF for N7 of adenine in $tRNA^{Phe}$. Symbols represent reactivity towards diethyl pyrocarbonate.

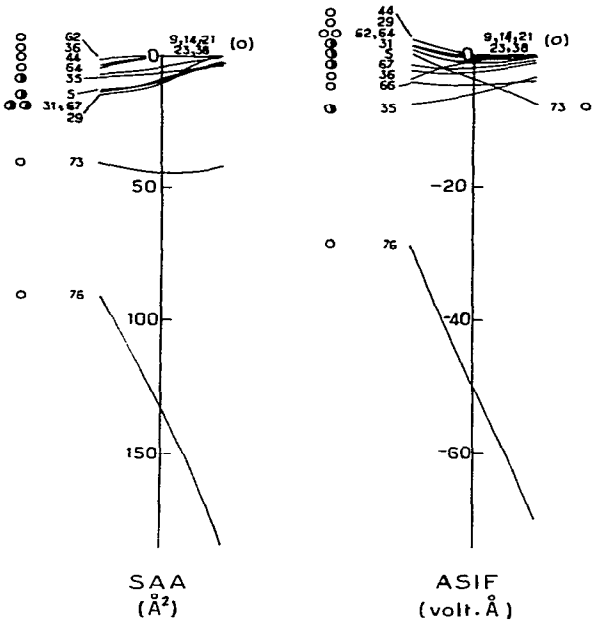

Fig. 9. Accessibility and ASIF for N6 of adenine in $tRNA^{Phe}$. Symbols represent reactivity towards 1-fluoro-2,4-dinitrobenzene.

the exact nature of the attacking species or the products of this interaction were not fully characterized [33]. We are consequently again obliged to study a range of probe radii for this reagent, although it is possible that an appropriate value for its model sphere would be close to that obtained previously for the phenyl cation, 2.8 Å. Experimentally the strongest reactivity is at adenine 76, but this interaction involves the sugar at either O3′ or O2′, rather than the base moiety. One base, adenine 35, was found to be quite reactive (36%) and three others (nos. 5, 31 and 67) to be slightly reactive. The calculated indices for N6 of adenine, shown in fig. 9, indicate that the largest value of both accessibility and ASIF is that for adenine 76. Why reaction at this nucleotide takes place at the sugar rather than at the base cannot presently be explained as the positions of the O2′ hydroxyl proton and that of the O3′ hydroxyl proton of the residue 76 are unknown so that comparisons between the sugars of the macro-

molecule are impossible. It can be seen, however, that the second most reactive base, adenine 35, is associated with the second most negative ASIF value for radii of attacking spheres up to 3 Å which would correlate with its partial reactivity. Such favoring of this base is not visible by accessibility alone. The slightly reactive bases are not well positioned for either index, but their low reactivity may be associated with a partial denaturation of the macromolecule, thought to be possible by the authors of the experimental study [35].

3.4. Reactivity of cytosines in $tRNA^{Phe}$

The only available electrophilic reaction involving cytosine in yeast $tRNA^{Phe}$ is that with dimethyl sulfate [28], leading to an N3 methylation. Two bases are found to be reactive, cytosines 74 and 75. The calculated indices are given in fig. 10, using the radius of the attacking sphere previously determined for the reactive intermediate CH_3^+, 1.8 Å. In this case both accessibility alone and the ASIF index are in agreement, placing the two experimentally reactive bases at the largest values.

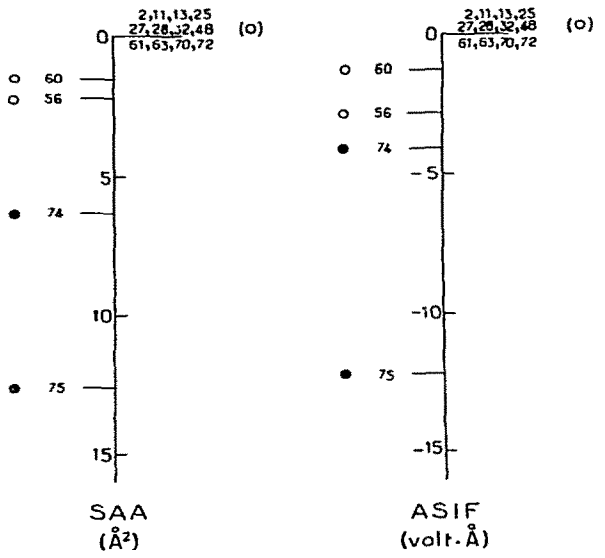

Fig. 10. Accessibility and ASIF for N3 of cytosine in $tRNA^{Phe}$. Symbols represent reactivity towards dimethyl sulfate.

3.5. Reactivity of uracils in $tRNA^{Phe}$

The reactivity of uracil and also of the modified base dihydrouracil has been studied in yeast $tRNA^{Phe}$ with carbodiimide [30], which in both cases carboethoxylates the N3 position. Only uracil 47 was fully reactive, while partial reactivities were observed for dihydrouracils 16 and 17 and for uracil 33. The theoretical results shown in fig. 11 demonstrate a good correlation between the experimental results and the ASIF index which attributes the most negative value to uracil 47 followed by both dihydrouracils. The accessibility values alone seem less satisfactory as the two dihydrouracils are both found to be more accessible than uracil 47.

For the range of attacking sphere radii chosen, uracil 33, which was found to be partially reactive, is inaccessible. However, below a radius of 1.4 Å this site is the first to become accessible, which would suggest that only a minor conformational

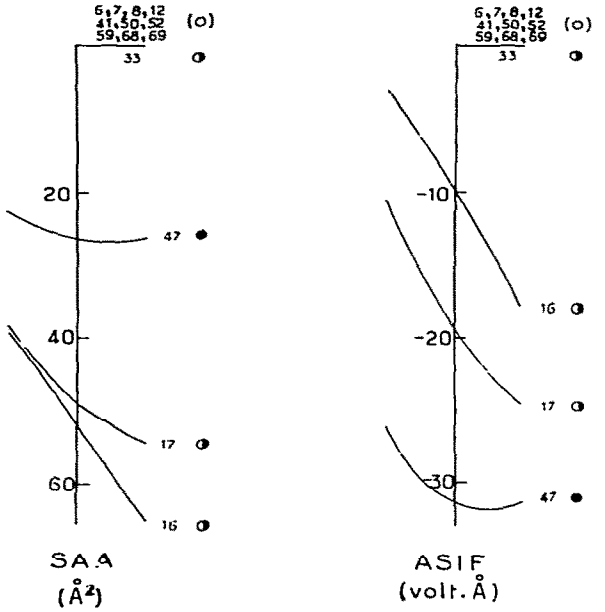

Fig. 11. Accessibility and ASIF for N3 of uracils and dihydrouracils in $tRNA^{Phe}$. Symbols represent reactivity towards carbodiimide.

change of the anticodon loop could render it available for reaction.

3.6. Reactivity of the phosphates in $tRNA^{Phe}$

The reactivity of the phosphates in yeast $tRNA^{Phe}$ has been assayed with ethylnitrosourea [34,35] which causes an ethylation of an anionic oxygen of the phosphate group. In fact, all the residues analysed (nos. 4–68) were found to be reactive, although to varying degrees. The problem of obtaining a correlation with a theoretical index may thus be expected to be more difficult than for contrasts between clearly reactive and unreactive sites. The results for the phosphate residues are shown in fig. 12, using an attacking sphere with the radius of 2.5 Å previously calculated for the ethyl cation. Because of the number of sites involved the representation has been changed to a graphic with the different phosphate residues indicated along the horizontal axis and the corresponding ASIF values by the left-hand and vertical axis and the solid line. The values indicated are in fact the average for the two anionic oxygens of each phosphate. The experimental reactivities are indicated by the right-hand axis and the dotted line.

Fig. 12 shows that a good overall agreement is achieved between reactivity and the ASIF index. The associated accessibilities are not shown on the present figure but they have been published previously for various attacking spheres [9,12] and they present altogether a similar correlation with the experimental results. The closeness of the results for the two indices is not surprising in this case as the anionic nature of the phosphate groups means that each residue is a source of very strong electrostatic field. Hence, the influence of the local environment of each residue on the electrostatic part of the ASIF index is relatively less important than that for the bases or sugars.

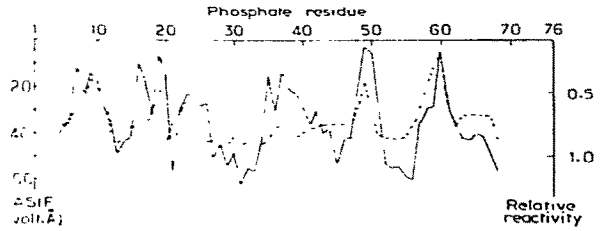

Fig. 12. ASIF and experimental reactivities for the phosphates of $tRNA^{Phe}$ towards ethylnitrosourea. ASIF values (left-hand ordinate and full line) are the average values for the two anionic oxygens of each residue. The experimental reactivities (from ref. 35) (right-hand ordinate and dotted line)are expressed as fractions representing the reduction in reactivity of each residue in passing from the unfolded to the native form of the macromolecule.

It is interesting to note that a statistical analysis of the quality of correlation obtained along the backbone of $tRNA^{Phe}$ shows that the least well reproduced experimental reactivities are those for phosphates 13, 14, 17, 18, 32, 34–36, 47 and 53. These residues are with two exceptions contained within the loops of the macromolecular structure (14, 17, 18 D loop, 32, 34–36, anticodon loop and 47, variable loop), regions whose conformation may be expected to change more easily in solution than that of the double-helical stems of the molecule.

4. Conclusions

The present study shows that an index of reactivity taking into consideration both the steric and electrostatic characteristics of the site examined in a macromolecule can better explain experimental reactivities than the sole consideration of steric accessibility. We have also been able to bring quantitative support to justify the representation of relatively complicated attacking species by spheres, provided appropriate radii are chosen and have shown how their optimal radii may be determined.

It must be recalled that the present work did not include conformational changes occurring in the macromolecule in solution or the effects of specific counterion interactions and that, moreover, only the electrostatic part of the energetics of interaction between the macromolecular site and a reactant has been considered. However, agreement with available experimental data shows that the proposed ASIF can be quite reliable especially in cases where the attacking reactive intermediate is known and is neither too large nor too flexible.

Acknowledgement

The authors wish to express their gratitude to the National Foundation for Cancer Research for supporting the present work.

References

1 B. Lee and F.M. Richards, J. Mol. Biol. 55 (1971) 379.
2 F.M. Richards, Annu. Rev. Biophys. Bioeng. 6 (1977) 151.
3 A. Shrake and J.A. Rupley, J. Mol. Biol. 79 (1973) 351–371.
4 C. Chothia, Nature 254 (1975) 304.
5 R. Lavery, A. Pullman and B. Pullman, Int. J. Quant. Chem. 20 (1981) 49.
6 P.K. Ponnuswamy and P. Thiyagarajan, Biopolymers 17 (1978) 2503.
7 C.J. Alden and S.-H. Kim, J. Mol. Biol. 132 (1979) 411.
8 C.J. Alden and S.-H. Kim, in: Nucleic acid geometry and dynamics, ed. R.H. Sarma (Pergamon Press, Oxford, 1980) p. 399.
9 R. Lavery, A. Pullman and B. Pullman, Theor. Chim. Acta 57 (1980) 233.
10 R. Lavery, A. Pullman, B. Pullman and M. de Oliveira, Nucleic Acids Res. 21 (1980) 5095.
11 S.R. Holbrook and S.-H. Kim, Biopolymers 22 (1983) 1145.
12 A. Pullman and B. Pullman, Q. Rev. Biophys. 14 (1981) 289.
13 A. Pullman and B. Pullman, Int. J. Quant. Chem. Quant. Biol. Symp. 7 (1980) 245.
14 B. Pullman, R. Lavery and A. Pullman, Eur. J. Biochem. 124 (1982) 229.
15 R. Lavery, A. Pullman and S. Corbin, in: Biomolecular stereodynamics, ed. R.H. Sarma (Adenine Press, New York, 1982) p. 185.
16 R. Lavery, A. Pullman and B. Pullman, Theor. Chim. Acta 62 (1982) 93.
17 R. Lavery and A. Pullman, in: New horizons in quantum chemistry (Reidel, Dordrecht, 1983) p. 439.
18 A. Pullman, B. Pullman and R. Lavery, J. Mol. Struct. 93 (1983) 85.
19 A.H. Stroud, in: Digital computer user's handbook, eds. M. Klerer and G.A. Korn (McGraw-Hill, New York, 1967) p. 2137.
20 G.N.J. Port and A. Pullman, FEBS Lett. 31 (1973) 70.
21 A. Pullman and D. Perahia, Theor. Chim. Acta 48 (1978) 29.
22 R. Lavery, A. Pullman and B. Pullman, Nucleic Acids Res. 8 (1980) 1061.
23 R. Lavery, M. de Oliveira and B. Pullman, J. Comp. Chem. 1 (1980) 301.
24 H. Berthod and A. Pullman, J. Chim. Phys. 62 (1965) 942.
25 Y.K. Kang, Ph.D. Thesis, Korea Advanced Institute for Science and Technology, Korea (1982).
26 R. Lavery, K. Zakrzewska and A. Pullman, J. Comput. Chem. (1983) in the press.
27 J.L. Sussman, J.B. Holbrook, R.W. Warant, G.M. Church and S.-H. Kim, J. Mol. Biol. 123 (1978) 607. [A further refined set of coordinates was actually employed in these calculates obtained as a personal communication from S.-H. Kim.]
28 D.A. Peattie and W. Gilbert, Proc. Natl. Acad. Sci. USA 77 (1980) 4679.
29 L. Litt, Biochemistry 8 (1969) 3249.
30 D. Rhodes, J. Mol. Biol. 94 (1975) 449.
31 F. Cramer, H. Doepner, F. van der Haar, F. Schlimme and H. Seidel, Proc. Natl. Acad. Sci. USA 61 (1968) 1384.
32 N.K. Kochetkov and E.I. Budovskii, Organic chemistry of nucleic acids, part B (Plenum Press, New York, 1971).
33 K. Watanabe and F. Cramer, Eur. J. Biochem. 89 (1978) 425.
34 V.V. Vlassov, R. Giege and J.-P. Ebel, FEBS Lett. 120 (1980) 12.
35 V.V. Vlassov, R. Giege and J.-P. Ebel, Eur. J. Biochem. 119 (1981) 51.